THE ASTROPHYSICAL JOURNAL SUPPLEMENT SERIES, 56:1–17, 1984 September

TIME SERIES INFRARED SPECTROSCOPY OF MIRA VARIABLES. II. CO $\Delta v = 3$ IN EIGHT MIRA VARIABLES AND ONE SRa VARIABLE

KENNETH H. HINKLE
Kitt Peak National Observatory[1]
WERNER W. G. SCHARLACH
National Radio Astronomy Observatory[2]
AND
DONALD N. B. HALL
Space Telescope Science Institute[3]
Received 1983 October 19; accepted 1984 February 28

ABSTRACT

The CO $\Delta v = 3$ lines have been analyzed in time series spectra of nine long-period variables. The CO $\Delta v = 3$ lines sample deep photospheric layers. Velocity, temperature, and column density derived from these lines are presented for each star as a function of phase. These data show that the photometric and spectroscopic variability of Mira variables is associated with an outwardly propagating wave, driven by a general stellar oscillation. This wave traverses the deep photosphere as a shock.

The program stars have periods ranging from 293 to 445 days and visual amplitudes from 2 to 8 mag. Eight stars are Mira-type variables. Among the Mira variables, the behavior of velocity, temperature, and column density with phase are similar, yet differences do exist from star to star, demonstrating that a family of objects has been sampled. One of the program stars, X Oph, is a semiregular (SRa) long-period variable. This star is undergoing stellar oscillations similar to those of the Mira variables, but with a lower amplitude. Implications of the observations for the origin of the SiO maser are discussed.

Subject headings: infrared: spectra — shock waves — stars: long-period variables — stars: pulsation

I. INTRODUCTION

The first paper of this series (Hinkle, Hall, and Ridgway 1982; hereafter Paper I) discussed time series infrared spectra of the Mira variable χ Cyg. The spectra were of the 1.5 to 2.5 μm and 4.6 μm regions. Analysis of the CO lines in these regions revealed a regularly pulsating photosphere and a complex circumstellar envelope. Most of the information on the photosphere came from the 1.5 to 1.8 μm CO second overtone ($\Delta v = 3$) bands. The information on the more extended atmospheric layers was from the 2.3 to 2.5 μm and 4.6 μm first overtone ($\Delta v = 2$) and fundamental ($\Delta v = 1$) bands.

The 1.6 μm CO $\Delta v = 3$ bands are an exceptionally valuable source of information on the photospheres of Mira variables. Since the $\Delta v = 3$ CO bands coincide with the 1.6 μm H^- opacity minimum, deep photospheric layers may be studied. The photometric variation at 1.6 μm is typically 1 to 2 mag (Catchpole *et al.* 1979), as compared with 5 or more magnitudes in the blue (Campbell 1955), making it possible to obtain high resolution spectra throughout the light cycle. Mira variables are among the brightest objects in the 1.6 μm sky. This allows extended wavenumber coverage in short integration times, even at minimum light.

Two separate lines of observational evidence show that the 1.6 μm infrared is probing much larger optical depths than in the blue and violet spectra. The most direct indication is the temperature. The assumption is made that temperature increases with increasing optical depth. Temperatures have been estimated in the visual by two methods. Blueviolet region atomic absorption lines (Buscombe and Merrill 1952) indicate excitation temperatures near 2500 K at maximum light in the prototype Mira o Cet. Spectral types estimated in the visual for o Cet range from M6e to M9e (Keenan, Garrison, and Deutsch 1974). Barnes (1973) suggests that the spectral type can be calibrated to the effective temperature ($T_{\rm eff}$) using the nonvariable M giant effective temperatures. The effective temperature scale of Dyck, Lockwood, and Capps (1974) gives a range of $T_{\rm eff}$ from 2900 K to 2150 K through the o Cet light cycle. These are contrasted to the 1.6 μm CO excitation temperatures for o Cet (§ III) which range from 4800 to 2800 K through the light cycle.

Velocity is the second indicator of optical depth. The 1.6 μm CO $\Delta v = 3$ lines exhibit a velocity behavior resulting from an outwardly propagating shock passing through the stellar atmosphere each cycle near maximum light (Paper I). A general stellar oscillation drives the shock (Wood 1979). On the other hand, the blueviolet absorption lines in Mira variables exhibit little change in velocity with time, showing

[1]Operated by the Association of Universities for Research in Astronomy, Inc., under contract with the National Science Foundation.
[2]Operated by Associated Universities, Inc., under contract with the National Science Foundation.
[3]Operated by the Association of Universities for Research in Astronomy, Inc., under contract with the National Aeronautics and Space Administration.

TABLE 1

PROGRAM STARS

Name	Period (days)	Spectral Type[a]	$v_{LSR} - v_{HC}$ (km s^{-1})	Number of Observations
R And ...	409	S5/4.5e	5.0	9
R Aql ...	284	M6.5e	17.5	8
R Cas ...	431	M7e	7.9	16
T Cas	445	M7.5e	7.3	5
T Cep ...	388	M6.5e	13.4	19
o Cet	332	M5.5e	−9.9	13
χ Cyg ...	407	S6+/1e	18.0	28[b]
R Leo ...	313	M7e	−7.3	12[c]
X Oph ...	334	M6.5e	18.0	14

[a]At maximum light, from Keenan 1966 and Keenan and Boeshaar 1980.

[b]Twenty seven observations from Hinkle, Hall, and Ridgway 1982 (Paper I).

[c]Nine observations from Hinkle 1978.

typical infall velocities of 5 to 10 km s^{-1} (Joy 1954). The blueviolet absorption lines must sample infalling gas in the oscillating atmosphere at all times. This implies that at least at phases when expanding gas is seen in the infrared (phases ~ -0.1–0.4), the blueviolet spectra must be exterior to the 1.6 μm line forming region.

The failure of the blueviolet region spectra to show periodic velocity changes while showing changes in line intensities (Merrill 1960; Joy 1954) makes the infrared spectra of particular interest. The shock, which emerges into the 1.6 μm photosphere near phase 0.7 (Paper 1), does result in the hydrogen emission lines in the visual spectrum near maximum light (Willson 1976; Hinkle and Barnes 1979; Wood 1979). However, the infrared spectra provide the only direct method of observing the atmospheric layers involved in stellar pulsation. The 1.6 μm spectra of χ Cyg (Paper I) and R Leo (Hinkle 1978) show a velocity variation that has an amplitude of tens of kilometers per second and is well correlated with the visual phase.

In this supplement we examine the CO $\Delta v = 3$ spectra of seven long-period variables whose infrared spectra have not been analyzed previously: R And, R Aql, R Cas, T Cas, T Cep, o Cet, and X Oph. New spectra are measured for R Leo and previous measurements (Hinkle 1978) are reanalyzed. A new χ Cyg spectrum has been measured and added to the results from Paper I. Table 1 lists the program stars, their spectral types, and periods.

The program stars are with one exception classical Mira variables. The terminology followed in this paper is that a Mira variable is a late-type giant of regular $\sim 10^2$–10^3 day period with visual light amplitude greater than 2.5 mag (Kukarkin *et al.* 1969). The non-Mira program star is X Oph which has a visual photometric amplitude of ~ 2 mag. The small amplitude is frequently (incorrectly) attributed to the presence of a bright K giant companion. As will be shown, this star is a SRa variable, a class of stars similar to the Mira variables, but with visual light amplitudes less than 2.5 mag. Both the SRa and Mira stars fall under the broader category of long-period variables (LPVs).

The program stars were selected because they are bright in the infrared. The mean K-band magnitude is ~ -1.5. R And is the faintest member of the set by ~ 1 mag, having a K-band magnitude of $\sim +0.3$. The majority of the stars also were selected because they are far north and may be observed most of the year during daytime. The following stars were included in the sample for special reasons. R And was selected because it is a northern S-type Mira. R Aql is a bright Mira with variable period. o Cet was observed as a result of a request for monitoring by McLean (1979). The R Leo observations were a follow up on the observations by Hinkle (1978). X Oph was included in our program because it is one of the few LPVs with a normal companion.

The following section reviews data acquisition and analysis. A discussion of the individual stars forms the third section. In the fourth section we discuss implications for masers. The conclusion section presents a general overview of the observational results. We have purposely limited the discussion in this supplement and have concentrated on a presentation of the data. A more thorough discussion of the implications of these and other observations will be presented in another paper in this series.

II. OBSERVATION AND REDUCTION

The data consist of 124 spectra obtained for the most part between 1976 June and 1980 October. Previously unreported observations account for 88 of the spectra. These are detailed in Tables 2A–2H, where the date of observation, visual phase calculated from the AAVSO light curves (Mattei 1981), signal-to-noise ratio, and resolution may be found. A description of the nine spectra of R Leo taken from Hinkle (1978) is given in his paper. Twenty-seven of the χ Cyg spectra are discussed in Paper I.

R Leo spectra discussed by Hinkle (1978) and 1972 and 1973 o Cet spectra were obtained with the JPL Fourier transform spectrometer (FTS) at the coudé focus of the McDonald Observatory 2.7 m telescope (Beer, Norton, and Seaman 1971). The other spectra were observed with one of two spectrometers at the Kitt Peak 4 m telescope. Between January 1976 and August 1978 a prototype spectrometer similar to the instrument described by Ridgway and Capps (1974) was used. In 1978 September the prototype was replaced by a more versatile and efficient spectrometer (Hall *et al.* 1979) which has been used for all subsequent observations.

Paper I discusses the photometric accuracy, frequency calibration, and line profile of the Kitt Peak instruments. Beer, Norton, and Seaman (1971) and Hinkle (1978) discuss the JPL instruments. To summarize, the photometric accuracy and frequency calibration of the spectra are limited by noise rather than instrumental characteristics. The frequencies of all points in a spectrum are referenced to the spectrometer laser frequency. After the laser frequency has been corrected for the index of refraction of air, the spectral frequencies require only a small (~ 1 km s^{-1}) correction for collimation differences between the reference and signal beams.

All the spectra discussed in this paper have been apodized using function I2 of Norton and Beer (1976). The Kitt Peak prototype spectrometer had instrumental apodization which resulted from systemic variation in reimaging onto the beam splitter with path length. We choose to convolve these spectra

TABLE 2A

TWO MICRON REGION SPECTRA OF R ANDROMEDAE

Date	JD (2,440,000+)	Visual Phase	S/N[a]	Resolution[a] (theoretical FWHM)	Integration Time (minutes)
1976 Jun 9	2939.2	0.54	94	0.16	57
1976 Sep 30 ...	3051.9	0.80	61	0.16	35
1976 Nov 8	3090.8	0.89	59	0.08	95
1976 Dec 6	3118.7	0.96	...[b]	0.15	65
1977 May 29 ...	3293.3	0.37	76	0.08	76
1977 Aug 26 ...	3381.9	0.58	85	0.08	60
1978 May 27 ...	3656.1	0.24	107	0.08	127
1978 Oct 17 ...	3798.8	0.58	114	0.07	67
1979 Jun 13	4038.1	0.16	86	0.07	91

[a]Spectra apodized by Norton and Beer 1976, function I2.
[b]No reverse scan.

TABLE 2B

TWO MICRON REGION SPECTRA OF R AQUILAE

Date	JD (2,440,000+)	Visual Phase	S/N[a]	Resolution[a] (theoretical FWHM)	Integration Time (minutes)
1976 Jun 7	2937.0	0.18	82	0.12	32
1976 Aug 18 ...	3008.7	0.43	110	0.12	63
1976 Sep 30 ...	3051.7	0.58	97	0.12	63
1977 Feb 19 ...	3194.2	0.08	54	0.08	33
1977 Jun 24	3318.9	0.53	63	0.08	33
1977 Aug 26 ...	3381.6	0.75	99	0.08	60
1977 Oct 2	3418.6	0.89	121	0.08	61
1978 Nov 8	3821.5	0.29	58	0.08	68

[a]Spectra apodized by Norton and Beer 1976, function I2.

TABLE 2C

TWO MICRON REGION SPECTRA OF R CASSIOPEIAE

Date	JD (2,440,000+)	Visual Phase	S/N[a]	Resolution[a] (theoretical FWHM)	Integration Time (minutes)
1976 Apr 7	2876.3	0.30	80	0.08	32
1976 May 13 ...	2912.2	0.39	...[b]	0.12	22
1976 Jun 6	2936.3	0.44	97	0.08	39
1976 Jul 25	2985.1	0.56	111	0.08	31
1976 Sep 29 ...	3050.9	0.71	83	0.08	35
1976 Nov 8	3090.7	0.81	94	0.08	40
1976 Dec 6	3118.6	0.87	127	0.08	61
1977 Jan 11	3155.4	0.96	116	0.08	30
1977 Feb 8	3183.3	0.03	112	0.08	30
1977 Feb 19 ...	3194.3	0.05	62	0.08	30
1977 Mar 28 ...	3231.3	0.14	56	0.08	31
1977 Aug 26 ...	3381.8	0.49	188	0.08	59
1977 Oct 2	3418.7	0.57	201	0.08	61
1978 May 23 ...	3652.2	0.12	156	0.08	69
1979 Feb 8	3913.3	0.72	259	0.07	79
1980 Feb 27 ...	4297.4	0.61	119	0.07	51

[a]Spectra apodized by Norton and Beer 1976, function I2.
[b]No reverse scan.

TABLE 2D

TWO MICRON REGION SPECTRA OF T CASSIOPEIAE

Date	JD (2,440,000+)	Visual Phase	S/N[a]	Resolution[a] (theoretical FWHM)	Integration Time (minutes)
1976 May 13 ...	2912.2	0.21	101	0.12	24
1976 Jun 9	2939.2	0.28	66	0.12	29
1976 Jul 25	2985.1	0.38	61	0.12	20
1979 Jun 13	4038.1	0.73	106	0.07	56
1982 Nov 6	5279.7	0.53	174	0.07	51

[a]Spectra apodized by Norton and Beer 1976, function I2.

TABLE 2E

TWO MICRON REGION SPECTRA OF T CEPHEI

Date	JD (2,440,000+)	Visual Phase	S/N[a]	Resolution[a] (theoretical FWHM)	Integration Time (minutes)
1976 Apr 11 ...	2880.2	0.72	113	0.08	30
1976 May 14 ...	2913.1	0.80	167	0.12	43
1976 Jun 8.....	2938.1	0.87	66	0.08	15
1976 Aug 18 ...	3008.8	0.04	78	0.08	32
1976 Sep 29 ...	3050.8	0.15	72	0.08	36
1976 Nov 6	3088.7	0.25	54	0.08	33
1976 Dec 5	3118.5	0.33	56	0.08	60
1977 Jan 11	3155.4	0.42	66	0.08	31
1977 Feb 19 ...	3194.3	0.53	68	0.08	30
1977 Mar 28 ...	3231.2	0.62	34	0.08	31
1977 May 30 ...	3294.1	0.78	157	0.08	60
1977 Jun 24	3319.0	0.85	104	0.08	32
1977 Aug 26 ...	3381.7	0.01	124	0.08	60
1977 Oct 2	3418.7	0.10	148	0.08	59
1977 Nov 30 ...	3478.4	0.25	106	0.08	33
1978 May 23 ...	3652.1	0.69	148	0.08	64
1978 Dec 9	3851.5	0.18	79	0.06	81
1979 Feb 8	3913.3	0.33	218	0.07	82
1980 Feb 27 ...	4297.2	0.29	139	0.07	25

[a]Spectra apodized by Norton and Beer 1976, function I2.

TABLE 2F

TWO MICRON REGION SPECTRA OF *o* CETI

Date	JD (2,440,000+)	Visual Phase	S/N[a]	Resolution[a] (theoretical FWHM)	Integration Time (minutes)
1972 Dec[b].....	1682.6 1675.6 1674.6	0.60	40	0.14	250
1973 Oct[b]	1957.8 1956.8 1955.9	0.42	65	0.14	418
1976 Sep 29 ...	3050.9	0.70	75	0.08	28
1976 Nov 5	3087.9	0.81	94	0.08	46
1979 Nov 2	4179.9	0.05	153	0.07	17
1980 Jan 4	4242.7	0.24	211	0.07	42
1980 Feb 27 ...	4297.4	0.40	211	0.07	33
1980 Jun 3.....	4394.2	0.69	102	0.07	20
1980 Jun 24	4415.2	0.75	122	0.07	17
1980 Aug 26 ...	4478.0	0.94	213	0.07	17
1980 Sep 1	4484.1	0.96	139	0.07	25
1980 Sep 22 ...	4505.1	0.02	202	0.07	17
1980 Oct 30 ...	4542.9	0.13	156	0.07	17

[a]Spectra apodized by Norton and Beer 1976, function I2.
[b]Data taken at McDonald Observatory.

TABLE 2G

TWO MICRON REGION SPECTRA OF χ CYGNI

Date	JD (2,440,000+)	Visual Phase	S/N[a]	Resolution[a] (theoretical FWHM)	Integration Time (minutes)
1980 Feb 27 ...	4297.1	0.24	153	0.07	17

[a]Spectra apodized by Norton and Beer 1976, function I2.

TABLE 2H

TWO MICRON REGION SPECTRA OF R LEONIS

Date	JD (2,440,000+)	Visual Phase	S/N[a]	Resolution[a] (theoretical FWHM)	Integration Time (minutes)
1976 Jun 17	2946.5	0.08	87	0.08	14
1980 May 25 ...	4385.5	0.73	83	0.06	48
1982 Nov 26 ...	5300.1	0.64	172	0.07	35

[a]Spectra apodized by Norton and Beer 1976, function I2.

TABLE 2I

TWO MICRON REGION SPECTRA OF X OPHIUCHI

Date	JD (2,440,000+)	Visual Phase	S/N[a]	Resolution[a] (theoretical FWHM)	Integration Time (minutes)
1976 Apr 11 ...	2880.1	0.31	90	0.08	40
1976 May 16 ...	2915.1	0.42	86	0.09	30
1976 Jun 20	2949.7	0.53	71	0.08	31
1976 Nov 7	3090.5	0.97	59	0.08	39
1977 Feb 8	3183.3	0.26	110	0.08	63
1977 Feb 19 ...	3194.2	0.29	51	0.08	29
1977 Mar 28 ...	3231.1	0.41	...[b]	0.08	30
1977 May 30 ...	3294.0	0.60	85	0.08	31
1977 Jun 24	3318.8	0.68	72	0.08	30
1977 Aug 25 ...	3380.6	0.87	55	0.08	30
1977 Aug 26 ...	3381.6	0.88	73	0.08	32
1977 Nov 30 ...	3478.3	0.17	31	0.08	32
1978 Oct 16 ...	3798.5	0.14	145	0.07	69
1980 Feb 27 ...	4297.1	0.67	111	0.07	34

[a]Spectra apodized by Norton and Beer 1976, function I2.
[b]No reverse scan.

and the spectra taken with the other spectrometers with the apodizing function to obtain uniform line profiles throughout the entire set of data and to increase the signal-to-noise in the spectra. Apodizing, in smoothing the sidelobes of the instrumental profile, reduces the resolution and increases the signal-to-noise. For function I2 the resolution is reduced 40%, and the signal-to-noise is increased by the same amount.

The instrumental apodization of the prototype FTS has not been taken into account in Table 2, so the actual resolution is ~10% inferior to the theoretical values listed for spectra taken with the KPNO prototype FTS. All the spectra listed in Table 2 cover the range 4000–6600 cm^{-1} which includes the CO $\Delta v = 2$ and $\Delta v = 3$ vibration-rotation bands. The signal-to-noise ratios are for the rms noise compared to the peak signal. Typically the peak signal occurs near 4600 cm^{-1}. The signal-to-noise in the CO $\Delta v = 3$ region (5550–6420 cm^{-1}) is less by up to a factor of 2, the actual amount depending on the phase-dependent energy distribution. While the spectra analyzed in this paper do not represent the highest quality data presently obtainable, the typical signal-to-noise ratios of 100 and spectral resolution of 4 km s^{-1} at 6000 cm^{-1} are well suited to the type of analysis we have undertaken.

The measurement of the spectra was carried out in the same way described in Paper I. "Average" line profiles were constructed from a short list of typically unblended lines. Using the velocity of the lowest point in the average line profile, a computer program measured the depths of all the $^{12}C^{16}O$ $\Delta v = 3$ lines. The least blended lines were selected from plots of these depths as a function of J'' for each branch of each band. The velocity of the deepest point of each of the least blended lines was measured. The mean velocity and uncertainty for each spectrum derived from the least blended lines

TABLE 3A

RESULTS FROM R ANDROMEDAE SPECTRA

Date	Radial Velocity	Excitation Temperature	Column Density
1976 Jun 9	−14.83 ± 0.22	2500 ± 200	24.67 ± 0.12
1976 Sep 30 ...	−8.26 ± 0.34	2100 ± 100	24.42 ± 0.07
1976 Nov 8	−4.90 ± 0.20	2000 ± 100	23.99 ± 0.15
1976 Dec 6	−5.66 ± 0.29	2000 ± 200	24.02 ± 0.15
	−29.27 ± 0.28	4400 ± 200	23.07 ± 0.20
1977 May 29 ...	−21.55 ± 0.12	2900 ± 100	24.42[a]
1977 Aug 26 ...	−13.39 ± 0.13	2800 ± 200	24.54 ± 0.11
1978 May 27 ...	−10.62 ± 0.38	1800:	22.72 ± 0.30
	−28.83 ± 0.13	3000 ± 100	24.47 ± 0.07
1978 Oct 17 ...	−14.57 ± 0.13	2800 ± 100	24.52 ± 0.10
1979 Jun 13	−10.57 ± 0.27	1800 ± 100	23.62 ± 0.25
	−28.68 ± 0.09	3600 ± 100	23.77 ± 0.05

[a] Column density uncertainties are relative to this observation.

TABLE 3B

RESULTS FROM R AQUILAE SPECTRA

Date	Radial Velocity	Excitation Temperature	Column Density
1976 Jun 7	+22.89 ± 0.12	3300 ± 100	23.66[a]
1976 Aug 18 ...	+32.39 ± 0.19	3100 ± 100	23.71 ± 0.05
1976 Sep 30 ...	+37.44 ± 0.21	3200 ± 200	23.36 ± 0.05
1977 Feb 19 ...	+20.78 ± 0.19	3600 ± 200	23.66 ± 0.05
1977 Jun 24	+34.48 ± 0.18	3200 ± 200	23.58 ± 0.04
1977 Aug 26 ...	+38.76 ± 0.26	3100 ± 100	23.42 ± 0.04
1977 Oct 2	...	...	...[b]
1978 Nov 8	+27.21 ± 0.15	3200 ± 200	23.66 ± 0.05

[a] Column density uncertainties are relative to this observation.
[b] Individual CO $\Delta v = 3$ lines not observable. $\Delta v = 3$ band heads and $\Delta v = 2$ lines are present.

TABLE 3C

RESULTS FROM R CASSIOPEIAE SPECTRA

Date	Radial Velocity	Excitation Temperature	Column Density
1976 Apr 7	+13.87 ± 0.16	3200 ± 200	23.87 ± 0.07
1976 May 13 ...	+17.14 ± 0.35	2800 ± 200	23.73 ± 0.10
1976 Jun 6	+18.46 ± 0.47	3000:	23.60 ± 0.30
	+22.53 ± 0.26	...[a]	...[a]
1976 Jul 25	+23.66 ± 0.25	3400 ± 400	23.55 ± 0.20
1976 Sep 29 ...	+27.87 ± 0.20	3400 ± 400	23.59 ± 0.10
1976 Nov 8	+30.36 ± 0.23	3200 ± 200	23.58 ± 0.08
1976 Dec 6	+31.67 ± 0.23	3000 ± 200	23.42 ± 0.10
1977 Jan 11	+29.96 ± 0.25	3000 ± 400	23.50 ± 0.15
	+4.11 ± 0.23	4000 ± 200	23.57 ± 0.25
1977 Feb 8	+28.48 ± 0.24	2700 ± 200	23.00 ± 0.10
	+5.90 ± 0.22	3800 ± 200	23.42 ± 0.08
1977 Feb 19 ...	+27.81 ± 0.34	2400 ± 200	23.10 ± 0.18
	+6.35 ± 0.26	3800 ± 100	23.43 ± 0.10
1977 Mar 28 ...	+26.50 ± 0.30	2400 ± 200	23.13 ± 0.14
	+8.27 ± 0.16	3800 ± 100	23.85[b]
1977 Aug 26 ...	+20.40 ± 0.21	3400 ± 200	23.75 ± 0.10
1977 Oct 2	+24.25 ± 0.26	2600:	23.52 ± 0.08
1978 May 23 ...	+29.38 ± 0.28	2700 ± 100	23.15 ± 0.14
	+9.14 ± 0.17	3800 ± 100	23.49 ± 0.04
1979 Feb 8	+25.32 ± 0.21	2900 ± 200	23.69 ± 0.10
1980 Feb 27 ...	+24.76 ± 0.21	3500:	23.64 ± 0.10

[a] Too few unblended lines present in spectrum to determine excitation temperature.
[b] Column density uncertainties are relative to this observation.

TABLE 3D

RESULTS FROM T CASSIOPEIAE SPECTRA

Date	Radial Velocity	Excitation Temperature	Column Density
1976 May 13 ...	−19.07 ± 0.24	3300 ± 200	24.09 ± 0.10
1976 Jun 9	−16.70 ± 0.17	3000 ± 200	24.27 ± 0.05
1976 Jul 25	−12.08 ± 0.32	2800 ± 200	24.14 ± 0.08
1979 Jun 13	−0.22 ± 0.30	2600 ± 200	23.22 ± 0.05
	−14.42 ± 0.12	3200 ± 100	23.79 ± 0.07
1982 Nov 6	−8.01 ± 0.14	3000 ± 100	24.04[a]

[a] Column density uncertainties are relative to this observation.

TABLE 3E

RESULTS FROM T CEPHEI SPECTRA

Date	Radial Velocity	Excitation Temperature	Column Density
1976 Apr 11 ...	−4.91 ± 0.17	2800 ± 100	23.34 ± 0.12
	−16.27 ± 0.17	3700 ± 100	23.42 ± 0.07
1976 May 14 ...	−3.29 ± 0.34	2600 ± 200	23.13 ± 0.12
	−17.22 ± 0.23	3600 ± 200	23.71 ± 0.05
1976 Jun 8	−2.39 ± 0.27	2800 ± 200	22.93 ± 0.20
	−19.19 ± 0.16	3600 ± 200	23.83 ± 0.10
1976 Aug 18 ...	−4.47 ± 0.32	2600:	22.24 ± 0.20
	−22.79 ± 0.10	3200 ± 200	24.04 ± 0.05
1976 Sep 29 ...	−20.20 ± 0.12	3200 ± 200	24.08 ± 0.05
1976 Nov 6	−18.30 ± 0.10	3200 ± 200	24.01 ± 0.07
1976 Dec 5	−16.64 ± 0.12	3200 ± 200	24.07 ± 0.05
1977 Jan 11	−14.80 ± 0.12	3400 ± 200	23.86 ± 0.08
1977 Feb 19 ...	−12.51 ± 0.13	3100 ± 200	24.14 ± 0.06
1977 Mar 28 ...	−10.90 ± 0.24	3000 ± 200	24.04 ± 0.05
1977 May 30 ...	−4.99 ± 0.28	2900 ± 100	23.19 ± 0.08
	−18.68 ± 0.17	4800 ± 300	23.07 ± 0.03
1977 Jun 24	−3.78 ± 0.22	2700 ± 200	22.59 ± 0.15
	−19.85 ± 0.12	3700 ± 200	23.84 ± 0.07
1977 Aug 26 ...	−24.13 ± 0.08	3600 ± 200	23.86 ± 0.08
1977 Oct 2	−22.96 ± 0.08	3600 ± 200	24.11 ± 0.12
1977 Nov 30 ...	−18.82 ± 0.12	3300 ± 200	24.24 ± 0.10
1978 May 23 ...	−7.26 ± 0.25	2900 ± 200	23.47 ± 0.08
	−17.81 ± 0.15	3800 ± 200	23.39 ± 0.10
1978 Dec 9	−20.74 ± 0.11	3200 ± 200	24.19 ± 0.08
1979 Feb 8	−15.71 ± 0.11	3100 ± 200	23.99[a]
1980 Feb 27 ...	−18.02 ± 0.12	3400 ± 200	24.09 ± 0.08

[a] Column density uncertainties are relative to this observation.

TABLE 3F

RESULTS FROM o CETI SPECTRA

Date	Radial Velocity	Excitation Temperature	Column Density
1972 Dec.....	+62.7 ± 0.3	2900 ± 300	23.55 ± 0.15
1973 Oct	+59.0 ± 0.1	3100 ± 300	23.81 ± 0.08
1976 Sep 29 ...	+63.52 ± 0.18	3100 ± 200	23.45 ± 0.07
1976 Nov 5	+65.85 ± 0.26	2800:	23.55 ± 0.10
1979 Nov 2	+67.59 ± 0.26	2900 ± 200	22.80 ± 0.05
	+47.67 ± 0.17	4200 ± 200	23.62 ± 0.07
1980 Jan 4	+51.89 ± 0.07	3600 ± 200	23.55[a]
1980 Feb 27 ...	+55.54 ± 0.09	3200 ± 100	23.43 ± 0.10
1980 Jun 3	+64.62 ± 0.13	3100 ± 200	23.63 ± 0.08
1980 Jun 24	+65.24 ± 0.16	3100 ± 200	23.67 ± 0.05
1980 Aug 26 ...	+68.59 ± 0.19	3000 ± 150	23.55 ± 0.20
1980 Sep 1	+67.85 ± 0.21	3000 ± 300	23.27 ± 0.12
	+44.74 ± 0.30	4800:	22.89 ± 0.12
1980 Sep 22 ...	+67.68 ± 0.15	3000 ± 300	23.10 ± 0.07
	+46.03 ± 0.12	4600 ± 200	23.28 ± 0.10
1980 Oct 30 ...	+66.28 ± 0.20	2900 ± 300	22.55 ± 0.10
	+48.10 ± 0.09	4000 ± 200	23.41 ± 0.14

[a] Column density uncertainties are relative to this observation.

TABLE 3G

RESULTS FROM χ CYGNI SPECTRA

Date	Radial Velocity	Excitation Temperature	Column Density[a]
1980 Feb 27 ...	-13.40 ± 0.07	3100 ± 100	24.30 ± 0.05

[a] Column density uncertainties are relative to 1977 Nov 30 (Hinkle, Hall, and Ridgway 1982).

TABLE 3H

RESULTS FROM R LEONIS SPECTRA

Date	Radial Velocity	Excitation Temperature	Column Density[a]
1976 Jun 17	-1.03 ± 0.11	3600 ± 200	23.59 ± 0.08
1980 May 25 ...	$+16.10 \pm 0.13$	3200 ± 200	23.57 ± 0.12
1982 Nov 26 ...	$+14.27 \pm 0.20$	3100 ± 100	23.63 ± 0.07

[a] Uncertainties relative to 1974 Jan spectrum (Hinkle 1978).

TABLE 3I

RESULTS FROM X OPHIUCHI SPECTRA

Date	Radial Velocity	Excitation Temperature	Column Density
1976 Apr 11 ...	-76.02 ± 0.14	3400 ± 100	23.37 ± 0.05
1976 May 16 ...	-73.56 ± 0.09	3400 ± 100	23.28 ± 0.04
1976 Jun 20	-72.01 ± 0.11	3200 ± 100	23.28 ± 0.03
1976 Nov 7	-77.72 ± 0.12	3400 ± 100	23.32[a]
1977 Feb 8	-77.61 ± 0.16	3300 ± 100	23.53 ± 0.04
1977 Feb 19 ...	-76.92 ± 0.15	3400 ± 100	23.53 ± 0.05
1977 Mar 28 ...	-74.10 ± 0.18	3600 ± 100	23.45 ± 0.05
1977 May 30 ...	-71.01 ± 0.16	3300 ± 100	23.22 ± 0.07
1977 Jan 24	-74.13 ± 0.11	3600 ± 100	23.16 ± 0.05
1977 Aug 25 ...	-76.49 ± 0.15	3400 ± 100	23.29 ± 0.03
1977 Aug 26 ...	-76.73 ± 0.11	3300 ± 200	23.40 ± 0.03
1977 Nov 30 ...	-78.69 ± 0.15	3500 ± 200	23.49 ± 0.05
1978 Oct 16 ...	-79.62 ± 0.10	3400 ± 200	23.39 ± 0.05
1980 Feb 27 ...	-67.10 ± 0.30	3300 ± 200	23.06 ± 0.08

[a] Column density uncertainties are relative to this observation.

is found in Tables 3A–3H. All velocities in this paper are heliocentric. The conversions to local standard of rest velocity have been included in Table 1.

A Gaussian function was fitted by least squares to the deepest two-thirds of the least blended lines. From plots of equivalent width versus central depth a calibration of equivalent width as a function of central depth was established. Equivalent widths derived from the central depths through this calibration were then used to construct curves of growth using the method of Hinkle, Lambert, and Snell (1976). The excitation temperature was found by minimizing the difference between the high and low excitation lines on the curve of growth.

Once the excitation temperature had been set, shifts between the curves of growth at different phases give the *variation* of CO column density with phase. Determining the absolute value of the column density at a given phase is a model-dependent problem. Ideally, a model atmosphere would be employed to synthesize the curve of growth. This approach is not possible for Mira variables since realistic model atmospheres are not available. To give a scale to the column density in Paper 1 the weak line portion of one of the curves of growth was fitted with an isothermal, plane-parallel model. By assuming similar atmospheric conditions among the program stars, we calibrated the column densities for the current paper from this curve of growth. Thus, the plots of the column density with phase have uncertainties of about ± 0.2 dex on a relative scale, but the calibration of the ordinate is uncertain by an order of magnitude or more. The excitation temperatures and column densities appear in Table 3.

III. INDIVIDUAL STARS

Each of the nine LPVs studied proved to have distinctive characteristics. In this section each star will be discussed separately. Visual light curves and infrared velocities, temperatures and column densities are presented in Figures 1–9. Note that near phase 0.0 ($\equiv 1.0$) both components in the double-lined data are shown in panel (*b*) of Figures 1–9. In panels (*c*) and (*d*) of Figures 1–9, one atmospheric region is followed through the light cycle, and the foldover at the beginning and end of the cycle has been eliminated to simplify the figure.

The SiO and CO thermal microwave lines originate in the circumstellar envelopes of late-type giants. These lines sample a circumstellar region that is both large compared to the stellar diameter and uniformly expanding. Morris (1980) demonstrated that in both the optically thin and thick case the systemic velocity is given by the center of the line profile and the expansion velocity by the edge of the line profile. Velocities determined in this manner are given for the program stars in Table 4. Table 5 gives velocities measured from blueviolet region absorption lines. As discussed in the introduction, these velocities are typically blueshifted 5–10 km s^{-1} from the systemic velocity.

a) *R Andromedae*

The visual and near-ultraviolet spectrum of this long-period (409[d]) S-type Mira variable is described by Merrill (1947*a*,1948) and Merrill and Greenstein (1955). Other than the presence of Tc lines (Merrill 1952), the R And green through near-ultraviolet spectrum is typical for a Mira variable, albeit S-type. The red to near-infrared spectrum has the notable property that the absorption lines double shortly after maximum light (Merrill and Greenstein 1958). Line doubling is never observed in the near-infrared spectra of oxygen-rich (M-type) Mira variables. The near-infrared spectra of oxygen-rich Mira variables are dominated by severely blended TiO bands which apparently obscure the atomic and CN spectrum in this region (Tsuji 1971).

Further analysis of the R And spectrum by Tsuji (1971) revealed that the atomic absorption lines in the 6000–9000 Å region were single at maximum light, doubling by phase 0.08. The red component has a velocity of -10.6 km s^{-1} at phases 0.08 and 0.13. This matches the velocity of the blueviolet absorption lines (Merrill 1947*a*). The blue component of the doubled lines has a velocity of -33.4 km s^{-1} at phase 0.08

TABLE 4

MICROWAVE THERMALLY EXCITED LINES

Star	Molecule ($v=0$)	Heliocentric Velocity	Expansion Velocity	Reference
R And	CO $J=1\rightarrow0$	-19 ± 0.5	10.5 ± 0.5	1
R Aql	SiO $J=2\rightarrow1$	$+31.2\pm0.8$	7.7 ± 1.3	2
R Cas	SiO $J=2\rightarrow1$	$+16.8\pm0.5$	8.9 ± 0.9	2,3
	SiO $J=2\rightarrow1$	$+14.1\pm2$	13 ± 1.5	4
	SiO $J=2\rightarrow1$	$+17.7$	7 ± 0.9	5
	SiO $J=2\rightarrow1$	$+16.4\pm0.8$	8.0 ± 1.0	6
	CO $J=1\rightarrow0$	$+16.9\pm2$	10.5 ± 2	4
o Cet	CO $J=1\rightarrow0$	$+51.9\pm0.5$	6 ± 0.5	1
	CO $J=1\rightarrow0$	$+54.9$	8	7
	CO $J=2\rightarrow1$	$+56.2\pm0.8$	4.9 ± 0.8	8
χ Cyg	SiO $J=2\rightarrow1$	-7.5 ± 0.6	7.5 ± 1.0	2
	SiO $J=2\rightarrow1$	-9 ± 2	7 ± 2	4
	SiO $J=2\rightarrow1$	-8.8	11.3 ± 0.9	5
	SiO $J=2\rightarrow1$	-6.0 ± 0.8	9.3 ± 1.0	6
	SiO $J=3\rightarrow2$	-9.2	16.1 ± 0.9	5
	SiO $J=3\rightarrow2$	-10.1 ± 0.5	...	9
	CO $J=1\rightarrow0$	-8.5 ± 0.5	8.5 ± 0.5	1
	CO $J=2\rightarrow1$	-8.5 ± 2.5	11.3 ± 2.5	8
R Leo	SiO $J=2\rightarrow1$	$+7.0\pm0.6$	3.9 ± 0.6	3
	SiO $J=2\rightarrow1$	$+7.8\pm0.4$	5.0 ± 0.7	2
	SiO $J=2\rightarrow1$	$+7.3\pm2$	3 ± 2.5	4
	SiO $J=2\rightarrow1$	$+6.4$	6.1 ± 0.9	5
	SiO $J=2\rightarrow1$	$+7.3\pm0.8$	6.2 ± 1.0	6
	SiO $J=3\rightarrow2$	$+8.2$	4.1 ± 0.6	5
	SiO $J=3\rightarrow2$	$+7.1\pm0.5$	...	9
	CO $J=2\rightarrow1$	$+6.3\pm1.0$	6.5 ± 1.0	8

REFERENCES:—(1) Lo and Bechis 1977. (2) Dickinson *et al.* 1978*a*. (3) Reid and Dickinson 1976. (4) Lambert and Vanden Bout 1978. (5) Wolff and Carlson 1982. (6) Olofsson *et al.* 1982. (7) Zuckerman 1981. (8) Knapp *et al.* 1982. (9) Schwartz, Zuckerman, and Bologna 1982.

TABLE 5

AVERAGE BLUEVIOLET REGION VELOCITIES

Star	Absorption	Emission	Circumstellar	Reference
R And ...	-11	-29	...	1,2
R Aql ...	$+34$	$+22$	$+23$	2,3,4
R Cas ...	$+23$	$+9$	$+13$	2,3,4,5
T Cas ...	-14	-25	...	2,5,6
T Cep ...	-12	-25	...	5,6
o Cet	$+60$	$+48$	...	7,8
χ Cyg ...	0	-15	-17	2,4,9,10,11
R Leo ...	$+14$	0	$+6$	2,4,6,11,12
X Oph ...	-71	-83	...	2,13,14

REFERENCES.—(1) Merrill 1947*a*. (2) Merrill 1941*b*. (3) Merrill 1945. (4) Wallerstein 1975. (5) Merrill 1941*a*. (6) Merrill 1952. (7) Joy 1954. (8) Wallerstein 1981. (9) Merrill 1947*b*. (10) Merrill 1953. (11) Sanner 1977. (12) Merrill 1946. (13) Merrill 1923. (14) Barnes and Fekel 1977.

and -32.3 at phase 0.13. The velocities from both components are in excellent agreement with the CO velocity curve (Fig. 1*b*). Similar agreement between velocities from near-infrared atomic absorption lines and 1.6 μm CO $\Delta v=3$ lines is reported for χ Cyg in Paper I. Hinkle and Barnes (1979) note in R Leo the CO $\Delta v=3$ and 1.6–2.5 μm atomic absorption-line velocities have nearly identical velocities. Evidently, the atomic lines from 0.7 to 2.5 μm sample the same region as the 1.6 μm CO.

Tsuji (1971) also determined excitation temperatures. The red component of the atomic lines at phase 0.08 had a temperature of 2100 ± 200 K. This is in good agreement with the CO excitation temperature for the infalling gas (phase 1.08) in Figure 1*c*. A red component is not seen in the CN. The blue component of the atomic lines had an excitation temperature of 2800 ± 150 K. From the blue component of the CN lines present at phase 0.08, a rotation temperature of ~4000 K was derived. In the blue component, the CN temperature is in fair agreement with the CO value (expanding gas at phase 0.08); however, the atomic value is too low. The excellent agreement of the velocities implies that CO, CN, and atomic lines are formed in the same atmospheric region. The ~1000 K temperature difference between the molecular and atomic species cannot represent a difference in the kinetic temperature and may reflect non–LTE populations in the atomic levels.

Masers from oxygen-bearing molecules (SiO, OH, and H_2O) would not be expected from S-type stars where the oxygen is

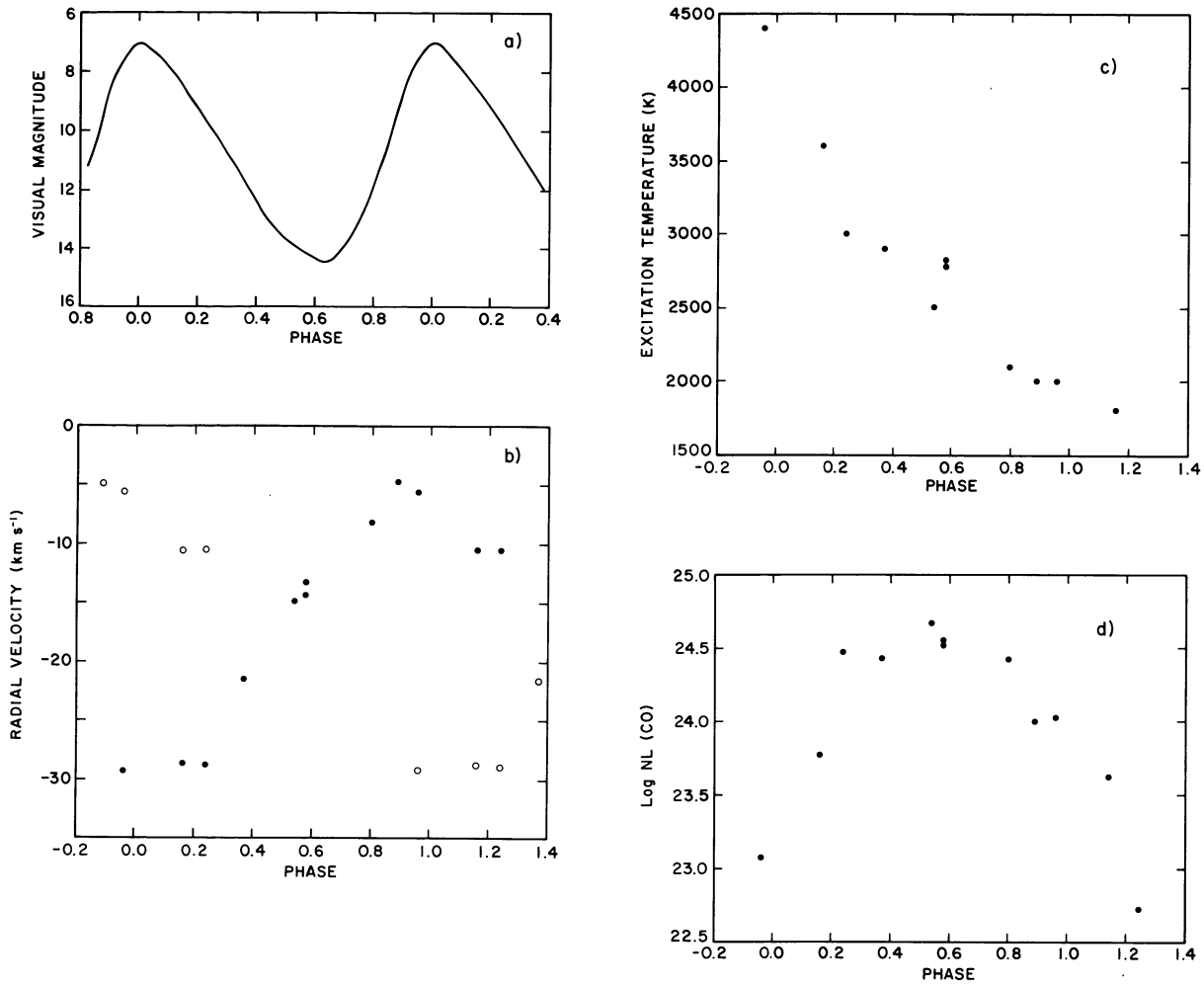

FIG. 1.—R And. (a) Average visual magnitude as a function of phase taken from Campbell (1955). (*b*) CO $\Delta v = 3$ radial velocities as a function of phase. Observations from several light cycles have been combined. Filled symbols show the evolution during a light cycle. Open symbols repeat the data backward and forward in time. Note that some phases are double-lined. (*c*) CO $\Delta v = 3$ excitation temperatures as a function of phase. As in (*b*), data from various light cycles are combined. Only the filled symbols in (*b*) are shown. (*d*) CO $\Delta v = 3$ column densities as a function of phase. As in (*b*), data from various light cycles are combined. Only filled symbols in (*b*) are shown.

mainly in CO (Scalo and Ross 1976). No masers have been detected from R And (Dickinson *et al.* 1978*b*). Thermal $v = 0$, $J = 1 \rightarrow 0$ CO of circumstellar origin has been observed, setting the systemic velocity at -19 km s^{-1} (Lo and Bechis 1977).

b) R Aquilae

Woodsworth and Hughes (1973) reported a 10.5 GHz radio flare with a peak flux of 240 mJy from R Aql. Bowers and Kundu (1979) detected a 14.9 GHz flux of 5.3 ± 2.0 mJy from R Aql. The emission was interpreted as a chromospheric or coronal signature. Kafatos, Michalitsianos, and Hobbs (1980) observed R Aql with *IUE* at phases 0.21 and 0.65. Both spectra contained the Mg II doublet in emission with the same intensity. This indicates the presence of 6000–8000 K gas which also was interpreted to be chromospheric or coronal. However, interpretation of the ultraviolet spectra must be done with caution because the gas behind the shock also produces Mg II emission (Willson 1976).

R Aql has a period which has been decreasing at a constant rate for at least 60 yr. The period was 320^{d} in 1915 and has shortened to 284^{d} in the 1976–1978 interval (Mattei 1981) when our observations were obtained. Wood (1975) and Wood and Zarro (1981) suggest that the period change is the result of a luminosity change associated with a helium-shell flash.

The microwave spectrum of R Aql has been well studied. SiO masers from the $v = 1$ $J = 1 \rightarrow 0$ and $J = 2 \rightarrow 1$ transitions have velocities of $+24$ to $+29$ km s^{-1} (Snyder and Buhl 1975; Spencer *et al.* 1981). Observations of microwave thermal SiO (Dickinson *et al.* 1978*a*) give a center of mass velocity of $+31$ km s^{-1} for R Aql. R Aql has a double peaked OH maser with velocities at $\sim +26$ and $+36$ km s^{-1} (Jewell *et al.* 1979). The average velocity of the double peaks in OH masers gives the systemic velocity (Reid 1976; Reid *et al.* 1977). For R Aql this agrees with the thermal SiO value of $+31$ km s^{-1}.

The infrared results are presented in Figure 2. Notably no double-lined observations were obtained despite the fairly extensive phase coverage. One spectrum at phase 0.89 has no

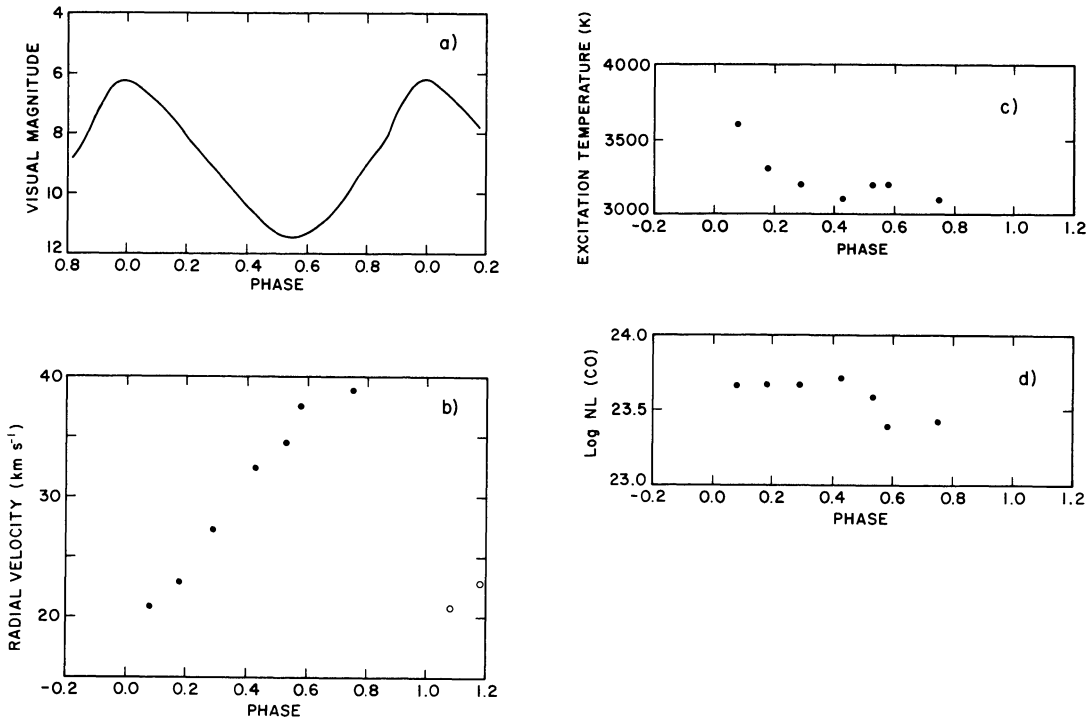

FIG. 2.—R Aql. (*a*)–(*d*) Same as Fig. 1.

measurable $\Delta v = 3$ CO lines. We interpret this as a phase when the column density of the infalling CO has become small and the emerging photosphere is too hot to form CO.

c) *R Cassiopeiae*

R Cas is one of the strongest stellar SiO maser sources. The $v = 1$ $J = 1 \rightarrow 0$ transition consists of multiple spectral components centered near $+19$ km s^{-1} (Moran *et al.* 1979). The maser is time variable in both intensity and velocity, with velocity components spread through the range $+11$–$+28$ km s^{-1} (Clark, Troland, and Johnson 1982). The R Cas SiO masers are known to originate spatially in spots smaller than 7 milli-arcsec (mas) diameter distributed in a cluster 20 mas diameter (Moran *et al.* 1979). 20 mas corresponds to approximately the expected stellar diameter (Paper I), 575 $R_\odot$, assuming a distance of 270 pc (Moran *et al.*).

Clark *et al.* (1981) discuss the $v = 2$ $J = 1 \rightarrow 0$, $v = 1$ $J = 2 \rightarrow 1$, and $v = 2$ $J = 2 \rightarrow 1$ SiO maser lines. At the epoch of our observations the $J = 2 \rightarrow 1$ lines had velocities peaked near 21–22 km s^{-1} and the $J = 1 \rightarrow 0$ velocities were near 15 km s^{-1}. Wolff and Carlson (1982) report detection of the $v = 1$ $J = 3 \rightarrow 2$ maser in R Cas. The levels populated in SiO masers strongly suggest that the maser is formed in a relatively high temperature region near the stellar photosphere (Clark *et al.* 1981; Elitzur 1980, 1981).

Thermal SiO and CO transitions also have been measured in the R Cas microwave spectrum (Table 4). These set the systemic velocity at $+16$ km s^{-1}. As was the case for R Aql, R Cas is a double-lined OH maser (Jewell *et al.* 1979). The systemic velocity derived from these lines is $+17$ km s^{-1}.

The infrared data are presented in Figure 3. The velocity curve (Fig. 3*b*) lacks the premaximum hook seen in most of the other CO $\Delta v = 3$ velocity curves. The temperature curve shows an abnormally large scatter. The large scatter is probably the result of blending of the CO lines with the exceedingly strong H_2O lines present in the R Cas spectrum near minimum light.

Flaud, Camy-Peyret, and Maillard (1977) discuss the 4000–10000 cm^{-1} R Cas spectrum observed at high resolution in 1972 December at phase 0.48. Their analysis of the CO utilizes the first overtone CO lines. As shown in Paper I the first overtone lines are blends with components formed in the second overtone line-forming region, in gas still falling in from the previous light cycle and in ~ 1000 K near-circumstellar gas. Flaud, Camy-Peyret, and Maillard did not realize the complexity of the spectrum since they observed a phase when the velocities of the components coincide and most lines appear single. Consequently, their analysis assumes a single component. They report a radial velocity of $+21.8$ km s^{-1} in reasonable agreement with our prediction of $+20.2$ at phase 0.48. Their excitation temperature of 2120 K is 1100 K lower than we predict. The temperature discrepancy is most likely the result of attempting to attribute one excitation temperature to lines from several distinct atmospheric regions.

d) *T Cassiopeiae*

T Cas is the longest period Mira variable in the sample. The infrared curves are undersampled (Fig. 4), but because line doubling is present as early as phase -0.28, the velocity curve is probably analogous to that of T Cep. Note, as in T Cep, that the light curve has a bump on the rising part.

A SiO $v = 1$ $J = 1 \rightarrow 0$ maser has been observed in T Cas at a velocity of -6 km s^{-1} (Spencer *et al.* 1981).

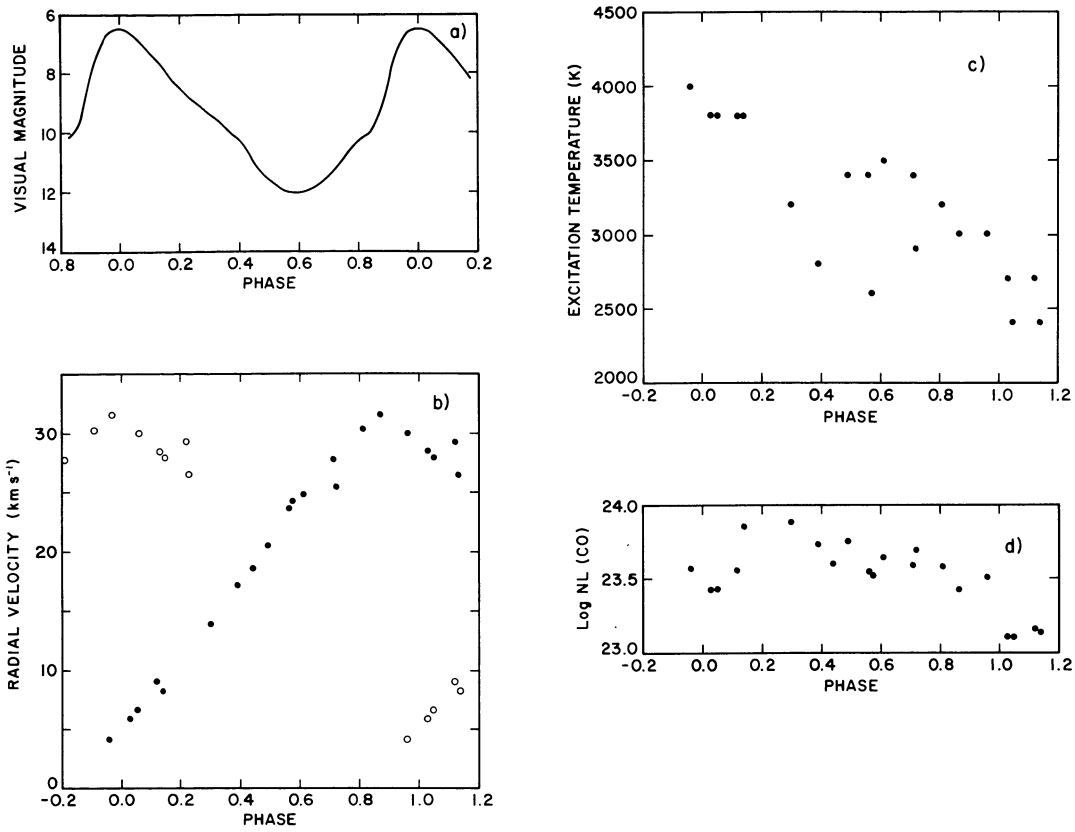

FIG. 3.—R Cas. (*a*)–(*d*) Same as Fig. 1.

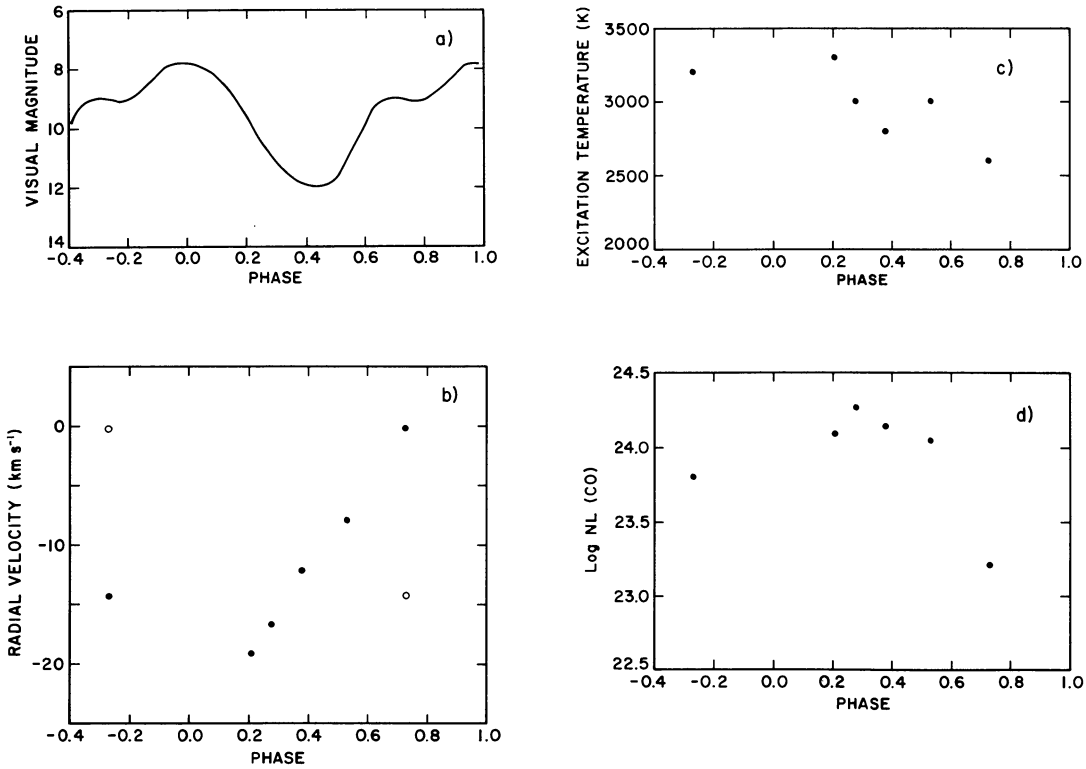

FIG. 4.—T Cas. (*a*)–(*d*) Same as Fig. 1.

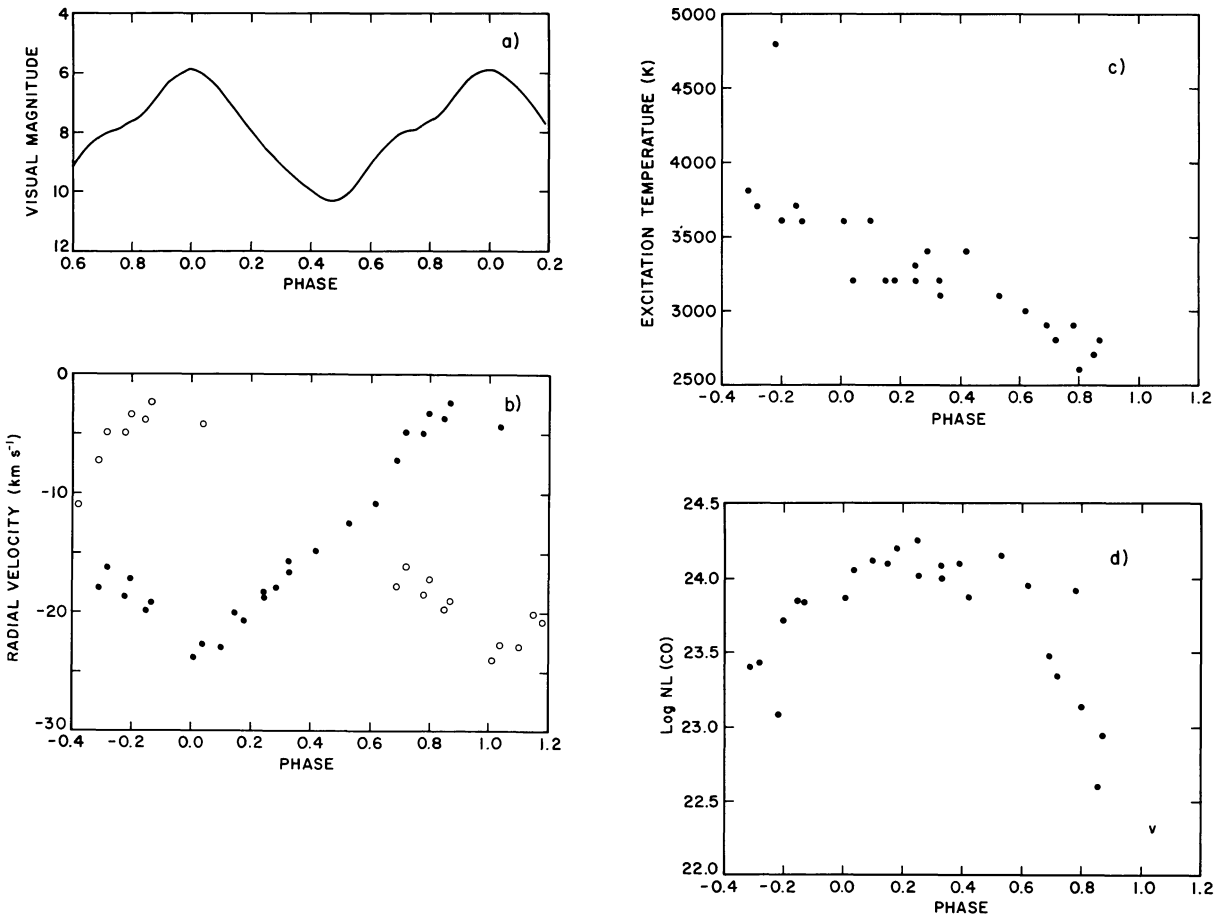

FIG. 5.—T Cep. (*a*)–(*d*) Same as Fig. 1.

e) *T Cephei*

The infrared data are presented in Figure 5*b*–5*d*. The doubling of the lines as early as phase −0.31 is remarkable. The premaximum blueshifted components form a striking hook in the velocity curve. The light curve has a conspicuous premaximum bump (Fig. 5*a*).

SiO masers have been observed in the $v=1$ $J=1\rightarrow 0$ and $J=2\rightarrow 1$ lines. They are at a velocity of ~ -16 km s^{-1} (Blair and Dickinson 1977; Spencer *et al.* 1981).

f) *o Ceti*

o Cet, the prototype Mira variable, is the brightest and most extensively studied star of its class. It is well known that o Cet is not a typical representative of the class because of the presence of a visually faint, peculiar Be companion (Joy 1926, Yamashita, Maihara, and Norimoto 1978). The binary has shown little motion since it was discovered in 1926. The currently favored orbital solution has a period of ~ 250 yr, setting the probable mass of the LPV component of the system at between 1 and 2 solar masses (Fernie and Brooker 1961).

There is evidence that the Be companion has an influence on at least the circumstellar shell of the LPV. Wallerstein (1981) was not able to find any of the circumstellar lines in the visual spectrum that are easily identifiable in other Mira-type stars. The CO $v=1$ $J=1\rightarrow 0$ thermal emission has a centroid at $+52$ km s^{-1} with a peculiar high peak at $+57$ km s^{-1} (Lo and Bechis 1977; Zuckerman 1981). All systemic velocities appearing in Table 4 are for the centroid of the emission ignoring the off-center spike. In all other Mira variables in which CO $v=10$ $J=1\rightarrow 0$ lines have been observed, the line has a symmetric line profile. Knapp *et al.* (1982) suggest on the basis of CO $v=0$ $J=2\rightarrow 1$ observations that o Cet's circumstellar envelope is optically thin and hot, characteristics they ascribe to the presence of the hot secondary.

A single-peaked 1665 MHz OH maser was reported by Dickinson, Kollberg, and Yngvesson (1975) at $+56.4$ km s^{-1}. As mentioned above, OH masers are generally double-peaked, with the peaks symmetric about the stellar center of mass velocity. A single-peaked maser cannot be construed to be proof of the interaction of the companion with the circumstellar shell since many single-peaked OH masers are known that cannot be shown to be binary stars. The OH maser is notable in that it is weak for a nearby oxygen-rich Mira. In fact, the OH maser, which is time variable, as are the OH masers in other Mira variables, is so weak that it has not been detected since 1975 (Olnon *et al.* 1980).

Elitzur (1981) presents arguments that the SiO masers in Mira variables are closer to the star than the OH or H_2O

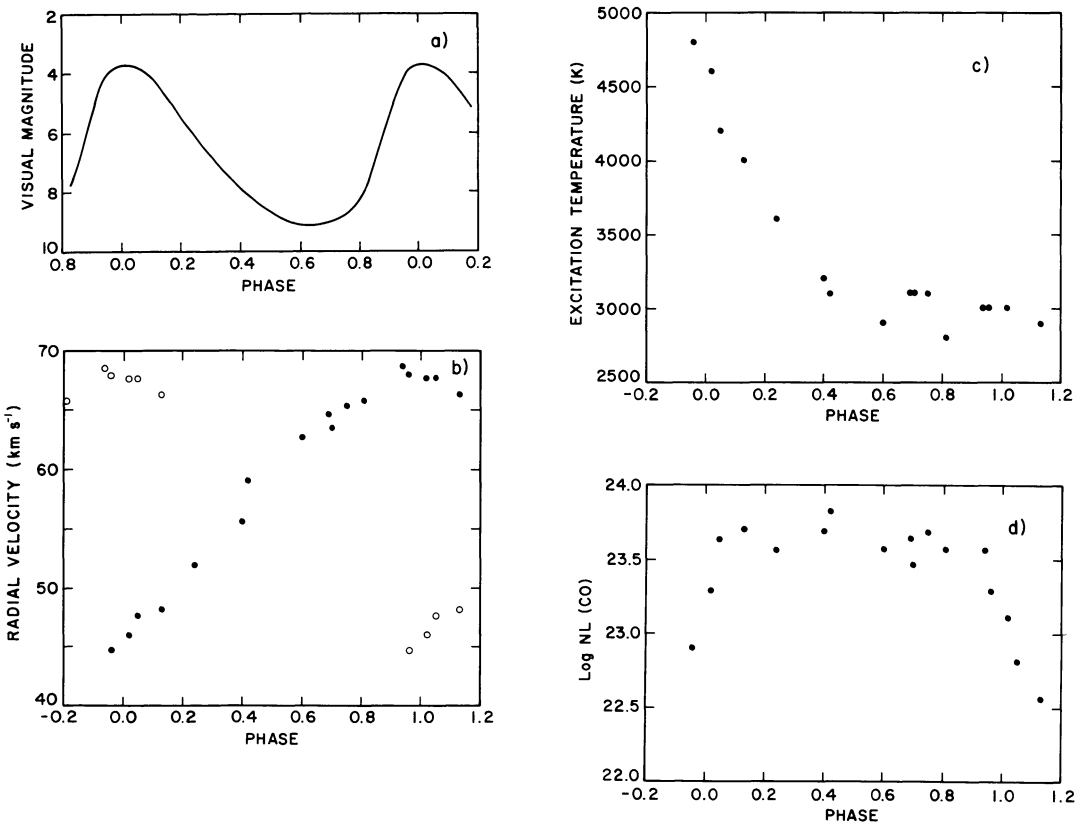

FIG. 6.—o Cet. (*a*)–(*d*) Same as Fig. 1.

masers. The o Cet SiO maser supports this argument since it does not seem affected by the companion. SiO masers are known from the $v=1$ $J=1\rightarrow 0$, $J=2\rightarrow 1$ and $v=2$ $J=1\rightarrow 0$ transitions (Synder and Buhl 1975; Hjalmarson and Olofsson 1979; Spencer *et al.* 1981). Velocities average $+57$ km s^{-1}.

The velocity, temperature, and column density curves (Figs. 6*b*–6*d*) have the same basic properties as previously seen in χ Cyg and R Leo with two notable differences. First, there is not a "hook" in the velocity curve at premaximum phases. Second, the velocity curve is depressed from phase 0.6–1.0 rather than linear from 0.1–0.8 as in previously studied Mira variables. Note that most of the data (Table 2F) comes from a single light cycle. The other Mira variables in this supplement are sampled over several light cycles. It may be that the small curvature in the velocity curve is a single-cycle variation (Paper I) that will not repeat in subsequent cycles.

Since Mira is a binary, the velocities were examined for motion about the barycenter. Orbital motion in the line of sight would increasingly displace the velocities from one cycle to the next. For the 8 yr interval folded together in Figure 6*b* no clear trend can be found. This places an upper limit of 5×10^{-9} km s^{-2} on the line of sight acceleration during this time period.

g) χ *Cygni*

Infrared velocities, temperatures, and column densities for 27 observations have been taken from Paper I. One new observation has been added. The data are plotted in Figure 7.

h) *R Leonis*

Infrared velocities and temperatures for R Leo are given by Hinkle (1978). We have used his data to calculate column densities. Four new observations have been added. All the data are plotted in Figure 8.

R Leo is a strong SiO maser. SiO $v=1$ $J=2\rightarrow 1$ maser velocities for this star range from -1 to $+14$ km s^{-1}. The time-averaged flux peaks near $+9$ km s^{-1} (Clark *et al.* 1984). The $v=1$ $J=1\rightarrow 0$ and $v=2$ $J=1\rightarrow 0$ masers also have been observed (Spencer *et al.* 1981). Wolff and Carlson (1982) detected the $v=1$ $J=3\rightarrow 2$ SiO maser. Clemens and Lane (1983) observed $v=1$ $J=5\rightarrow 4$. Schwartz, Zuckerman, and Bologna (1982) observed masers in the $v=2$ $J=3\rightarrow 2$ and $J=4\rightarrow 3$ transitions.

i) *X Ophiuchi*

Few Mira variables are known to have companions. X Oph is a member of an even smaller subset of Mira variables known to have "normal" companions, in this case a K1 giant (Merrill 1923). An obvious use of a normal companion is to set the absolute magnitude and distance to the Mira from the companion's absolute magnitude. In the case of X Oph, Fernie (1959) finds an M_V of $+1.1\pm 0.2$ for the K1 III companion, giving a distance modulus of 7.4. A reddening correction decreases the distance modulus to 6.9 ± 0.3 or 240 ± 35 pc.

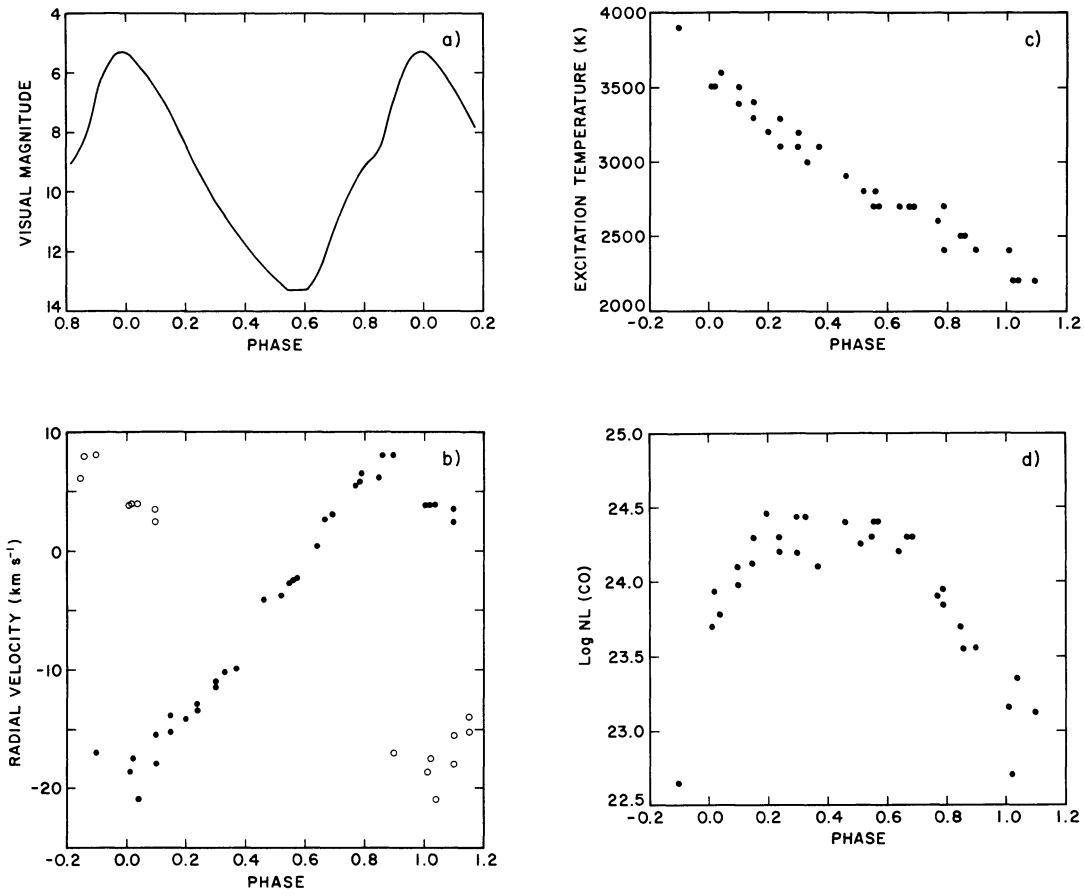

FIG. 7.—χ Cyg. (*a*)–(*d*) Same as Fig. 1.

The visual orbit has a period of ~ 500 yr (Fernie 1959). Merrill (1923) measured the velocity of the companion at -71 ± 3 km s^{-1}. This is equal to the LPV's absorption line velocity of -71 ± 2 km s^{-1} measured by Merrill at several maxima. The line-of-sight velocity difference between the stars implied by the orbit is only ~ 2 km s^{-1}. The agreement between velocities measured from the K giant spectrum and from absorption lines in the maximum light Mira spectrum was thus taken to mean that the systemic velocity of a Mira variable could be measured from the velocity of the absorption lines near maximum light (Feast 1970). Statistical analysis of OH maser velocities (Reid 1976) and observations of thermally populated circumstellar CO lines (Reid and Dickinson 1976) have shown that this is incorrect. It is now well established that the visual absorption lines of Mira variables are redshifted from the systemic velocity.

At minimum light the K1 III companion dominates the blueviolet spectrum of the system. The combined visual magnitude ranges from 6.9 to 8.6 during the light cycle (Campbell 1955). The K1 III apparent visual magnitude is estimated at 8.9 (Merrill 1923). However, in the 2 μm infrared the K1 III star does not contaminate the Mira spectrum at any phase. Taking the $V - K$ for a K1 giant to be 2.48 (Frogel *et al.* 1978), the K giant 2 μm magnitude is ~ 6.5 mag fainter than that of the Mira at minimum (Xhozov *et al.* 1978).

The infrared velocity curve of X Oph (Fig. 9*b*) is not typical of the other Mira variables studied. The amplitude is small, and the mean velocity of -73 km s^{-1} is in agreement with the velocity found from the visual absorption lines (Merrill 1923; Barnes and Fekel 1977). The visual amplitude of X Oph is small, 2.1 mag (Fig. 9*a*). This generally has been attributed to light from the companion dominating the light curve except at maximum light of the Mira. Observations at 1.04 μm reveal that X Oph is in fact a low-amplitude variable (Lockwood and Wing 1971). While no infrared velocity curves have been measured for low-amplitude late-type variables, Figure 9*b* would fit the expected results. In Figure 9*c*, the temperature variation during the cycle is too low to be measured. The conclusion is that the best-studied Mira with a normal companion is not a Mira at all but a SRa–type long-period variable.

The infrared spectra cover a period of 4 yr. If the Mira had appreciable motion about the barycenter of the system in this time period, the velocities from different cycles would be increasingly separated along the ordinate of Figure 9*b*. No orbital motion can be seen in our velocities. This is not surprising since comparison of velocities measured in the visual over a time span of 54 yr, similarly, gives no indication of orbital motion (Barnes and Fekel 1977).

IV. IMPLICATIONS FOR SiO MASER MODELS

Our results have some obvious implications in the understanding of where the SiO masers originate. There is a consensus that the other stellar masers, OH and H_2O, originate in

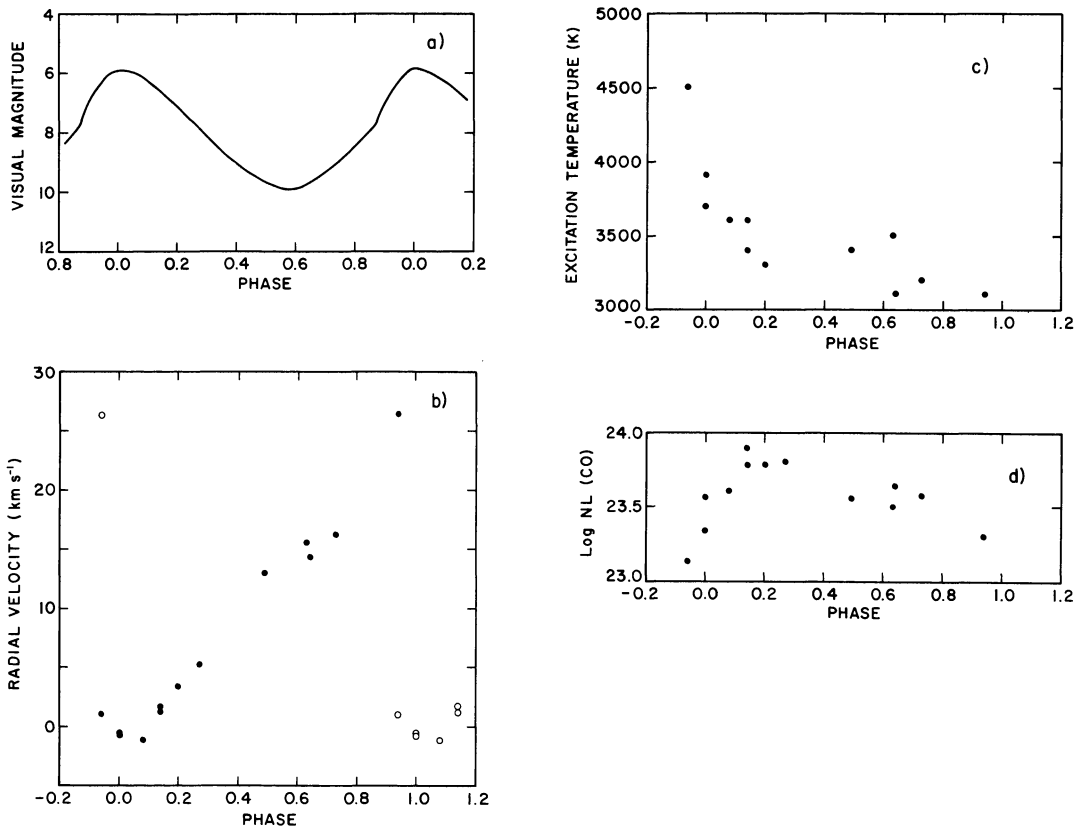

FIG. 8.—R Leo. (*a*)–(*d*) Same as Fig. 1.

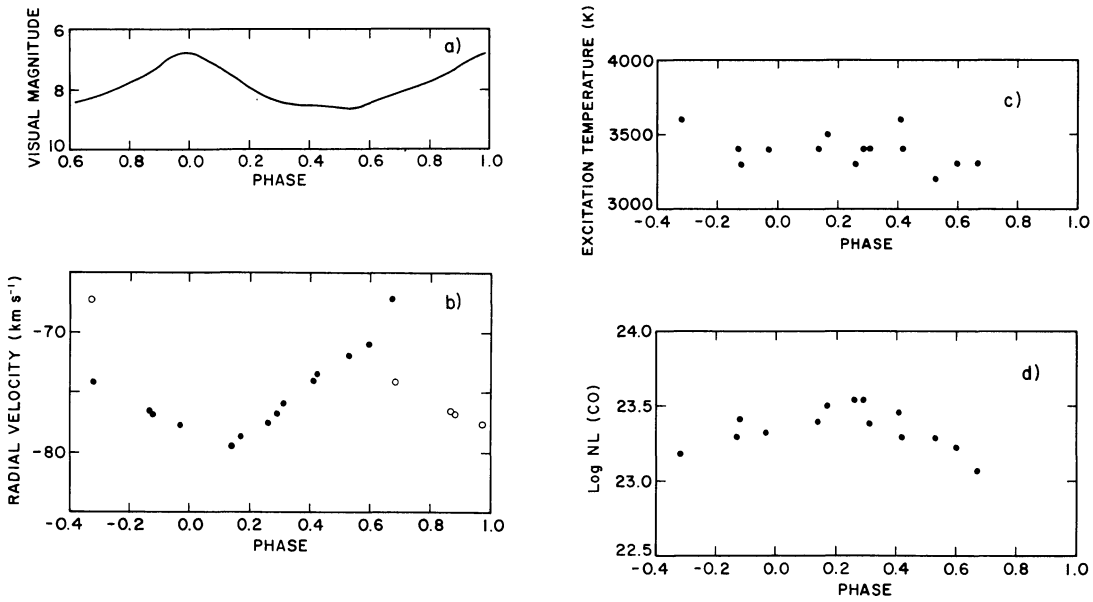

FIG. 9.—X Oph. (*a*)–(*d*) Same as Fig. 1.

circumstellar regions well removed from the hot pulsating layers seen in the 1.6 μm CO (Elitzur 1981), and these masers will not be discussed. Elitzur (1980, 1981), Clark, Troland, and Johnson (1982), and Clark *et al.* (1984) argue that the SiO masers must come from a hot region (~ 2000 K) near or actually in the 1.6 μm CO region. The principal argument in favor of this view is that the masers originate between rotational levels in excited vibrational levels. Several masers are seen in the $v = 2$ level (0.30 eV), and one maser is known in the $v = 3$ level (0.45 eV). As we have demonstrated, the 1.6 μm CO region undergoes large amplitude velocity changes during the light cycle. Clark *et al.* suggest tangential amplification to explain the lack of large amplitude velocity shifts in SiO masers. Changes in SiO maser line profiles near phase 0.9 are attributed to passage of the shock through the SiO maser forming region.

Problems arise in making any model fit the SiO maser observations. Lane (1982) provides a detailed discussion of the many constraints on the radiative transfer imposed by the observations of masers in excited levels. The infrared observations provide yet more constrains. In particular, our observations raise serious difficulties for an origin of the masers in the 1.6 μm CO line-forming region. The large-amplitude velocity and temperature changes during the light cycle result in large molecular column densities changes. The SiO column density changes will be more pronounced than the CO column density changes illustrated in panel (*d*) of Figures 1–9 since the dissociation energy is smaller (8.3 eV for SiO compared to 11.1 eV for CO). The maser observations appear to indicate nearly constant conditions throughout the light cycle. The change in SiO maser line profiles reported by Clark *et al.* near maximum light in R Cas is not as severe as we would expect from the CO temperature and column density data. Another objection to an origin for the SiO masers in the same region as the 1.6 μm CO comes from the continuous opacity, dominated in the infrared by H^-. H^- opacity increases significantly from 1.6 μm to 1 mm, so that the 1.6 μm CO line-forming regions are probably not observable at millimeter wavelengths.

Two experiments should be undertaken to establish where in the atmosphere the SiO maser originates. One is to undertake simultaneous infrared and microwave observations to see if any of the infrared velocity components, especially those seen at 2.3 and 5 μm, display velocity or column density changes that can be correlated with velocity or intensity changes observed in the maser. The second experiment is to undertake time series *VLBI* observations of sufficient spatial resolution to separate tangentially amplified components.

V. CONCLUSIONS

The Mira variables in our sample, while clearly individuals, share many characteristics. All of the second overtone CO velocity curves have the same basic shape, the essential features being a discontinuity during the premaximum phases and a linear portion of increasing velocity through minimum light. The temperature curves all show gas at excitation temperatures of ~ 3500 K or greater near maximum light with the temperature decreasing monotonically through the light cycle. The velocity and temperature curves indicate radial pulsation driving compression waves. Shocks develop before the emergence of the wave into the line forming layers. Paper I discusses the details of the atmospheric kinematics associated with the features of the velocity, temperature, and column density curves. This discussion will not be reviewed.

While all Mira variables studied show similarities in the behavior of the photospheric lines with phase, striking differences are present in the phase of line-doubling, range of excitation temperature, behavior of excitation temperature with phase, and the shapes and scale of the column density changes with phase. While each Mira is individually identifiable from the observations, two groups of Mira variables are notable. T Cep and T Cas have doubled CO lines near phase -0.4, have conspicuous bumps on their rising light curves, and have large (for non–S-type Mira variables) column densities. X Oph is a low-amplitude pulsator, not a "Mira" variable since the visual light amplitude is less than 2.5 mag, but shares some features of the T Cep group, in particular, early CO-doubling and the same shape column density curve. R Aql, R Cas, o Cet, and R Leo form a group of Mira variables, showing doubled CO lines near maximum light, and nearly identical column density versus phase curves. χ Cyg and R And, both S-type Mira variables seem related to this group, notwithstanding their huge CO column densities. A detailed discussion of the implications of the data on physical models for Mira atmospheres and pulsation will be presented in a later paper in this series.

The extended time series of observations analyzed in this paper could not have been obtained without the dedicated support of W. A. Lenz and J. C. Golson at the Mayall 4 m telescope. Dr. S. T. Ridgway provided support at the telescope and encouragement with the project. For the visual light curves and times of maxima of the LPVs, we are indebted to J. A. Mattei and the AAVSO observers.

REFERENCES

Barnes, T. G. 1973, *Ap. J. Suppl.*, **25**, 369.
Barnes, T. G., and Fekel, F. C. 1977, *Observatory*, **97**, 1.
Beer, R., Norton, R. H., and Seaman, C. H. 1971, *Rev. Sci. Instr.*, **42**, 1393.
Blair, G. N., and Dickinson, D. F. 1977, *Ap. J.*, **215**, 552.
Bowers, P. F., and Kundu, M. R. 1979, *A.J.*, **84**, 791.
Buscombe, W., and Merrill, P. W. 1952, *Ap. J.*, **116**, 525.
Campbell, L. 1955, *Studies of Long Period Variables* (Cambridge: AAVSO).
Catchpole, R. M., Robertson, B. S. C., Lloyd Evans, T. H. H., Feast, M. W., Glass, I. S., and Carter, B. S. 1979, *So. African Astr. Obs. Circ.*, **1**, 61.
Clark, F. O., Troland, T. H., and Johnson, D. R. 1982, *Ap. J.*, **261**, 569.
Clark, F. O., Troland, T. H., Lovas, F. J., and Schwartz, P. R. 1981, *Ap. J. (Letters)*, **244**, L99.
Clark, F. O., Troland, T. H., Pepper, G. H., and Johnson, D. R. 1984, *Ap. J.*, **276**, 572.
Clemens, D. P., and Lane, A. P. 1983, *Ap. J. (Letters)*, **266**, L117.
Dickinson, D. F., Kollberg, E., and Yngvesson, S. 1975, *Ap. J.*, **199**, 131.
Dickinson, D. F., Reid, M. J., Morris, M., and Redman, R. 1978*a*, *Ap. J. (Letters)*, **220**, L113.
Dickinson, D. F., Snyder, L. E. Brown, L. W., and Buhl, D. 1978*b*, *A.J.*, **83**, 36.
Dyck, H. M., Lockwood, G. W., and Capps, R. W. 1974, *Ap. J.*, **189**, 89.
Elitzur, M. 1980, *Ap. J.*, **240**, 553.

Elitzur, M. 1981, in *Physical Processes in Red Giants*, ed. I. Iben and A. Renzini (Dordrecht: Reidel), p. 363.
Feast, M. W. 1970, *Observatory*, **90**, 25.
Fernie, J. D. 1959, *Ap. J.*, **130**, 611.
Fernie, J. D., and Brooker, A. A. 1961, *Ap. J.*, **133**, 1088.
Flaud, J.-M., Camy-Peyret, C., and Maillard, J.-P. 1977, in *Les Spectres des Molecules Simples au Laboratoire et en Astrophysique, 21st Liège Internat. Ap. Symp.* (Liegè: Universite de Liegè), p. 246.
Frogel, J. A., Persson, S. E., Aaronson, M., and Matthews, K. 1978, *Ap. J.*, **220**, 75.
Hall, D. N. B., Ridgway, S. T., Bell, E. A., and Yarborough, J. M. 1979, *Proc. SPIE*, **172**, 121.
Hinkle, K. H. 1978, *Ap. J.*, **220**, 210.
Hinkle, K. H., and Barnes, T. G. 1979, *Ap. J.*, **234**, 548.
Hinkle, K. H., Hall, D. N. B., and Ridgway, S. T. 1982, *Ap. J.*, **252**, 697.
Hinkle, K. H., Lambert, D. L., and Snell, R. L. 1976, *Ap. J.*, **210**, 684.
Hjalmarson, Å., and Olofsson, H. 1979, *Ap. J. (Letters)* **234**, L199.
Jewell, P. R., Elitzur, M., Webber, J. C., and Snyder, L. E. 1979, *Ap. J. Suppl.*, **41**, 191.
Joy, A. H. 1926, *Ap. J.*, **63**, 281.
_____. 1954, *Ap. J. Suppl.*, **1**, 39.
Kafatos, M., Michalitsianos, A. G., and Hobbs, R. W. 1980, *Astr. Ap.*, **92**, 320.
Keenan, P. C. 1966, *Ap. J. Suppl.*, **13**, 333.
Keenan, P. C., and Boeshaar, P. C. 1980, *Ap. J. Suppl.*, **43**, 379.
Keenan, P. C., Garrison, R. F., and Deutsch, A. J. 1974, *Ap. J. Suppl.*, **28**, 271.
Knapp, G. R., Phillips, T. G., Leighton, R. B., Lo, K. Y., Wannier, P. G., Wootten, H. A., and Huggins, P. J. 1982, *Ap. J.*, **252**, 616.
Kukarkin, B. V., *et al.* 1969, *General Catalogue of Variable Stars* (Moscow: Sternberg State Astr. Inst.), p. A27.
Lambert, D. L., and Vanden Bout, P. A. 1978, *Ap. J.*, **221**, 854.
Lane, A. P. 1982, Ph.D. thesis, University of Massachusetts.
Lo, K. Y., and Bechis, K. P. 1977, *Ap. J. (Letters)*, **218**, L27.
Lockwood, G. W., and Wing, R. F. 1971, *Ap. J.*, **169**, 63.
Mattei, J. A. 1981, private communication.
McLean, I. S. 1979, *IAU Circ.*, No. 3407.
Merrill, P. W. 1923, *Ap. J.*, **57**, 251.
_____. 1941*a*, *Ap. J.*, **93**, 380.
_____. 1941*b*, *Ap. J.*, **94**, 171.
_____. 1945, *Ap. J.*, **102**, 347.
_____. 1946, *Ap. J.*, **103**, 275.
_____. 1947*a*, *Ap. J.*, **105**, 360.
Merrill, P. W. 1947*b*, *Ap. J.*, **106**, 274.
_____. 1948, *Ap. J.*, **107**, 303.
_____. 1952, *Ap. J.*, **116**, 21.
_____. 1953, *Ap. J.*, **118**, 453.
_____. 1960, in *Stars and Stellar Systems*, Vol. 6, *Stellar Atmospheres*, ed. J. L. Greenstein (Chicago: University of Chicago Press), p. 509.
Merrill, P. W., and Greenstein, J. L. 1955, *Ap. J. Suppl.*, **2**, 225.
_____. 1958, *Pub. A.S.P.*, **70**, 98.
Moran, J. M., Ball, J. A., Predmore, C. R., Lane, A. P., Huguenin, G. R., Reid, M. J., and Hansen, S. S. 1979, *Ap. J. (Letters)*, **231**, L67.
Morris, M. 1980, *Ap. J.*, **236**, 823.
Norton, R. H., and Beer, R. 1976, *J. Opt. Soc. Am.*, **66**, 259.
Olnon, F. M., Winnberg, A., Matthews, H. E., and Schultz, G. V. 1980, *Astr. Ap. Suppl.*, **42**, 119.
Olofsson, H., Johansson, L. E. B., Hjalmarson, Å., and Nguyen-Quang-Rieu. 1982, *Astr. Ap.*, **107**, 128.
Reid, M. J. 1976, *Ap. J.*, **207**, 784.
Reid, M. J., and Dickinson, D. F. 1976, *Ap. J.*, **209**, 505.
Reid, M. J., Muhleman, D. O., Moran, J. M., Johnston, K. J., and Schwartz, P. R. 1977, *Ap. J.*, **214**, 60.
Ridgway, S. T., and Capps, R. W. 1974, *Rev. Sci. Instr.*, **45**, 676.
Sanner, F. 1977, *Ap. J. (Letters)*, **211**, L35.
Scalo, J. M., and Ross, J. E. 1976, *Astr. Ap.*, **48**, 219.
Schwartz, P. R., Zuckerman, B., and Bologna, J. M. 1982, *Ap. J. (Letters)*, **256**, L55.
Snyder, L. E., and Buhl, D. 1975, *Ap. J.*, **197**, 329.
Spencer, J. H., Winnberg, A., Olnon, F. M., Schwartz, P. R., Matthews, H. E., and Downes, D. 1981, *A.J.*, **86**, 392.
Tsuji, T. 1971, *Pub. Astr. Soc. Japan*, **23**, 275.
Wallerstein, G. 1975, *Ap. J. Suppl.*, **29**, 375.
_____. 1981, *Pub. A.S.P.*, **93**, 453.
Willson, L. A. 1976, *Ap. J.*, **205**, 172.
Wolff, R. S., and Carlson, E. R. 1982, *Ap. J.*, **257**, 161.
Wood, P. R. 1975, in *IAU Colloquium 29, Multiple Periodic Variable Stars*, ed. W. S. Fitch (Dordrecht: Reidel), p. 69.
_____. 1979, *Ap. J.*, **227**, 220.
Wood, P. R., and Zarro, D. M. 1981, *Ap. J.*, **247**, 247.
Woodsworth, A., and Hughes, V. A. 1973, *Nature Phys. Sci.*, **246**, 111.
Xhozov, G. V., Xhudyakova, R. N., Parionov, V. M., and Parionova, P. V. 1978, *Trudy Astr. Obs. Leningrad*, **34**, 68.
Yamashita, Y., Maihara, H., and Norimoto, Y. 1978, *Pub. Astr. Soc. Japan*, **30**, 219.
Zuckerman, B. 1981, *A.J.*, **86**, 84.

DONALD N. B. HALL: Space Telescope Science Institute, Homewood Campus, Baltimore, MD 21218

KENNETH H. HINKLE: Kitt Peak National Observatory, P.O. Box 26732, Tucson, AZ 85726

WERNER W. G. SCHARLACH: National Radio Astronomy Observatory, 2010 N. Forbes Blvd., Tucson, AZ 85745